# Assessment of Precipitation Observations by a Heterogeneous Network of X- and K-band Radars

Stephen Frasier

Stephen J. Frasier[1], Fadela Kabeche[2], Jordi Figueras i Ventura[2], Hassan Al-Sakka[2], Pierre Tabary[2] , Jeff Beck[3], Olivier Bousquet[3]

[1]*Microwave Remote Sensing Laboratory, University of Massachusetts, Amherst, MA 01003, USA, frasier@ecs.umass.edu*

[2]*Centre de Météorologie Radar, Direction des Systèmes d'Observation, Météo-France, 42 Av Coriolis, 31057 Toulouse CEDEX, France*

[3]*Centre National de Recherches Météorologiques, Météo-France, 42 Av Coriolis, 31057 Toulouse CEDEX, France*

(Dated: 30 May 2012)

## 1. Introduction

The French Southern Alps area of Southeast France is a mountainous region prone to heavy rain and flash-flood events in the summer and autumn months. Because of the complex terrain, radar coverage by France's terrestrial network in this area is poor. Météo-France along with regional partners has established a project entitled ``Risques Hydrométéorologiques en Territoires de Montagnes et Méditerranéens'' (RHYTMME) that is deploying a network of four X-band polarimetric radars to improve the coverage in this region. At present, two radar sites are operational. One of these is a pre-existing installation located near Nice on Mont Vial. It is a Novimet Hydrix radar owned by Centre National de la Recherche Scientifiques (CNRS) and operated under contract by Novimet. This radar employs an offset parabolic reflector with no radome. The other radar, owned and operated by Météo-France, is located approximately 50 km to the Northeast on Mont Maurel. It is a Selex-Gematronik X-band radar employing a center-fed parabolic antenna with a radome. Of comparable size, power, and capability, the principle difference between the two X-band radars is the presence or lack of a radome.

Between these two sites, in the village of Puget-Théniers in the Var valley, a Metek K-band (24 GHz) micro-rain radar (MRR) was installed and operated for most of 2011 by the Centre National de Recherches Météorologiques (CNRM). The MRR provides vertical profiles of the Doppler spectrum due to precipitation, from which a variety of parameters are deduced. These include drop-size distribution, rain-rate, and reflectivity factor. Deriving these properties from the Doppler spectrum necessarily neglects the impacts of vertical air motion. Thus, the estimates obtained in convective precipitation may be subject to some error.

In this paper we use concurrent observations from these three radars to investigate impacts of wet radome attenuation on the Mont Maurel radar as well as the relationships between differential phase and path-integrated attenuation and differential attenuation. The following section describes the network and measurement methodology, while the subsequent sections describe respectively the principle studies conducted.

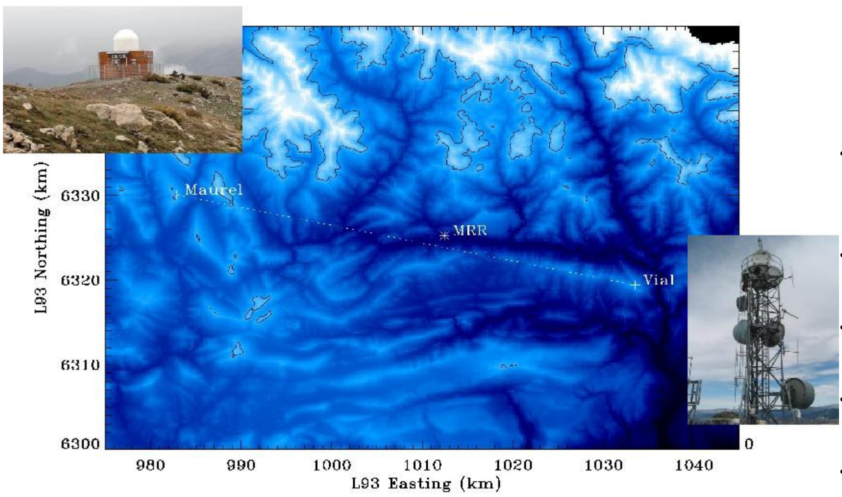


*Figure 1: Regional topography surrounding the two X-band radars: Mont Maurel (left) and Mont Vial (right)*

## .2. The Network

Figure 1 shows the relative locations of the three radars and the regional topography. The two X-band radars are separated by 52 km. The K-band MRR is located 22 km from Mont Vial and 30 km from Mont Maurel and nearly along the baseline between the two radars. While not equidistant from both X-band radars, the differing beamwidths of the two radars partially offset this effect (the site is closer to Mont Vial which has the wider beam). Thus, the sampling volumes of the two radars at this location are quite similar.

For this study we compare near-simultaneous observations by the two X-band radars over the MRR location. While the sampling volumes are nearly spatially matched, the differing scan patterns of the two radars yield time differences of up to 2.5 minutes (the tilts analyzed herein are repeated at 5 minute intervals). Thus, fast-moving features may be present in one radar's pixel and absent in other's. This temporal mismatch results in additional scatter of the comparison beyond that due to inherent fluctuation of the weather echo, but should not affect relative biases observed between the radars.

Observations by the MRR during 2011 were surveyed for episodes with reflectivity factors exceeding 45 dBZ at the altitudes of interest. A total of 14 days between April and November were selected, each consisting of 288 observations by each tilt of each of the X-band radars. Along the radials passing over the MRR site, we then selected 9 independent range bins for comparison. Only reflectivity factors exceeding 0 dBZ were considered.

## 3. Wet-Radome Attenuation

Figure 2 shows a color-coded histogram of all available observations. These are attenuation-corrected X-band reflectivity factors produced by the Météo-France dual-polarization processing chain (Figueras i Ventura et al., 2012). This histogram does not take into account the effect of the radome on the Maurel radar. Since the radar is deployed in a remote location at high elevation, reliable monitoring of the true rain rate at the radar site is difficult. We use the reflectivity observed at the nearest usable range bins to the Maurel radar as a proxy for the rain rate on the radar, and hence the relative wetting of the radome. In this case, we use the 6th range bin (between 1.5 and 2 km) along the radial passing over the MRR site. Denoting this reflectivity $Z_M$, we then stratify the observations of Vial and Maurel subject to $Z_M$ within a prescribed range. While this is clearly an imperfect measure of radome wetting, it is the most straightforward to derive from routine observations.

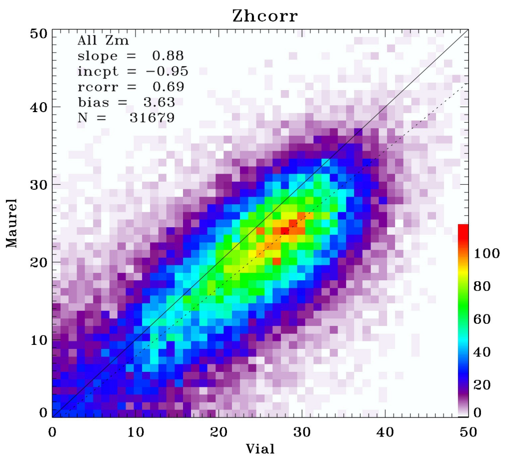


*Figure 2: Histogram of Maurel vs Vial Reflectivity over the site of the MRR*

Figure 3 shows histograms similar to Figure 2 except they are conditioned on particular ranges of $Z_M$ as indicated. One can observe an increasing bias between the two measurements as $Z_M$ increases. Performing this over a number of ranges of observed $Z_M$ yields the curve shown in Figure 3. This curve shows the average bias (Vial/Maurel) over all observed reflectivities as a function of the measured $Z_M$. For low values of $Z_M$ we assume a dry radome. Here we observe a bias between the two radars of approximately 2.5 dB. This difference includes an inter-radar calibration error (Note: based on this and other observations including QPE retrievals, the calibration constant of the Maurel radar has since been adjusted by 2 dB). More importantly, bias in excess of this amount for larger values of $Z_M$ is attributed to the 2-way attenuation through the (wet) radome. Because the measured $Z_M$ is subject to this attenuation, we add this bias to the measured $Z_M$ to obtain the intrinsic $Z_M$ which can then be related to the rain rate.

Radome performance is commonly specified by manufacturers in terms of one-way attenuation. Symbols in Figure 4 show the derived one-way attenuation vs rain-rate assuming either Marshall-Palmer (diamonds) or WSR-88D (triangles) Z-R relations. The dashed line shows the result obtained by Bechini et al., (2010) which were performed on a similar X-band radar. In their study, they used a disdrometer to obtain intrinsic reflectivities to compare to radome-attenuated X-band measurements at close range. They obtain a relationship proportional to $R^{1/3}$, consistent with theory for laminar water sheeting. The dotted line is a fit of the same form to the present observations yielding the empirical relation

$$A\ (\mathrm{dB}) = 0.2 + 0.85\, R^{1/3}$$

where A is the one-way attenuation and R is expressed in mm/hr. The solid line is the theoretical attenuation through a 2.5 m diameter radome with a uniform thickness of water at 20 C computed via the method described in Kurri and Huuskonen (2008). The dash-dot line is the relation obtained by Trabal et al. (2008). We have divided their result by two to obtain one-way attenuation, and we have added 0.3 dB to include dry radome attenuation.

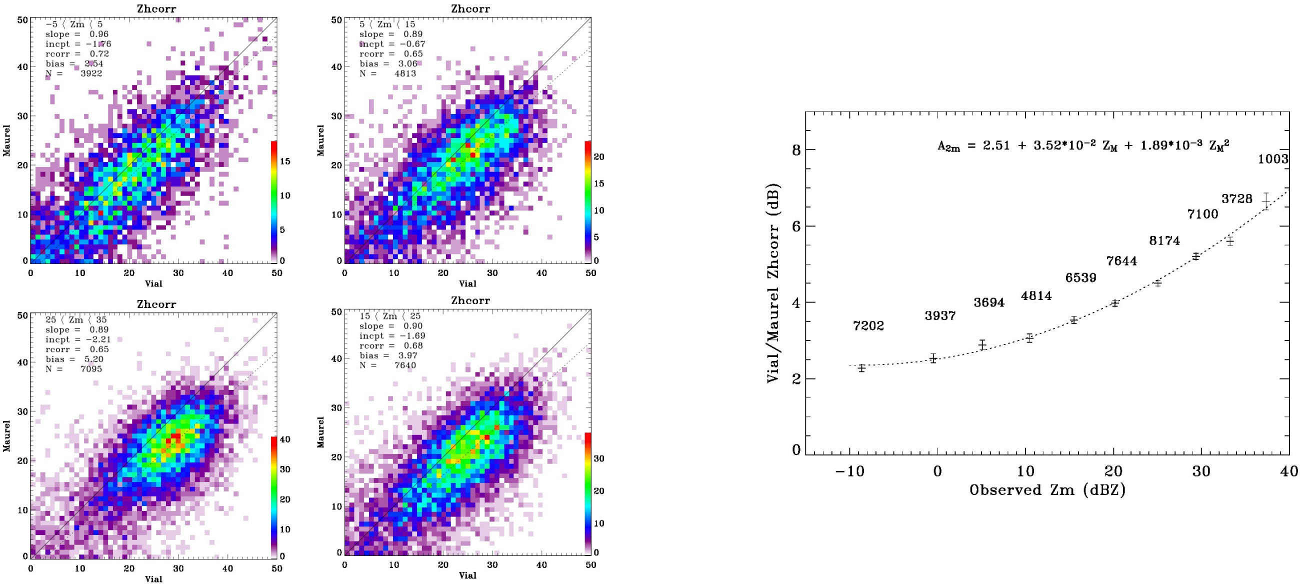


*Figure 3: On left, clockwise from upper left are Vial vs Maurel reflectivity conditioned on increasing values of reflectivity at the Maurel radar, $Z_M$. On right, Vial/Maurel bias is plotted vs $Z_M$. The number of samples is indicated over each point with the uncertainty of the estimate.*

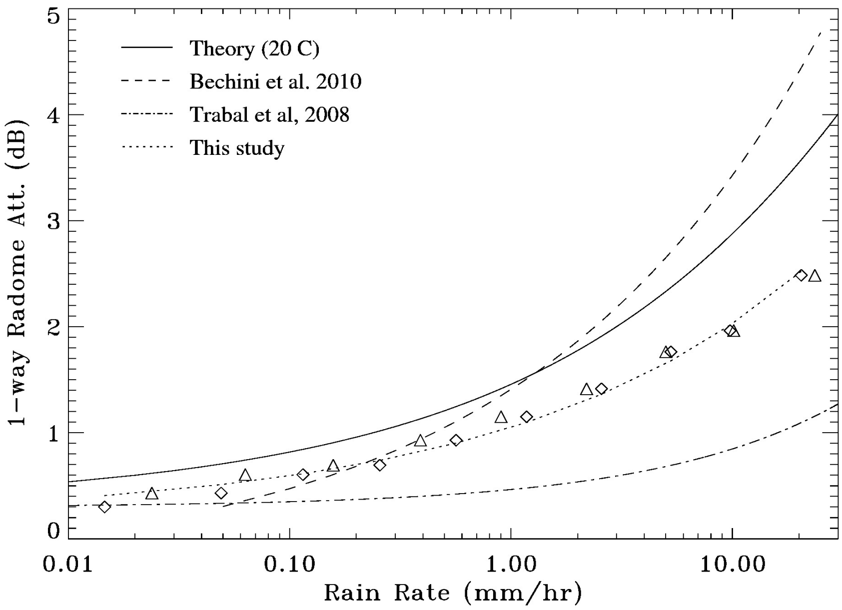


*Figure 4: One-way radome attenuation vs rain rate via Marshall-Palmer (diamonds) or WSR-88D (triangles) Z-R relationship.*

The present result falls somewhat below the theoretical prediction and signifcantly below the result of Bechini et al. (2010). They noted the radome used for their study was ``old'' and had lost its hydrophobic properties. The Maurel radar was installed in October 2010 and so was in its first year of service for the data collected in this study. It may exhibit better hydrophobic properties, though it has been indicated that radomes may lose their hydrophobic properties within the first six months to a year of service. Thus, the observed results appear reasonably consistent with expectations. Over time, one may reasonably expect that the radome attenuation will increase as the hydrophobic coating degrades. In the absence of any knowledge of the radome condition, the theoretical curve would seem to be an improvement on no compensation at all. Finally, we note the comparatively low radome attenuation obtained by Trabal et al., (2008). The data use in their study were collected in summer 2007 which was the first year of that network's observations. The radomes may have been 'newer' with better hydrophobic properties. The difference of the methodology used to derive the relationship may also contribute to the observed difference. They studied area extensive X-band reflectivities over a rain-gauge network and used nearby WSR-88D (S-band) observations over the X-band radar site as the indicator of local rain rate.

As an independent test, we assess the wet-radome correction by comparison to observations by the K-band MRR. Although the frequencies are quite different, the method employed by the MRR to calculate Z (from the 6th moment of the estimated DSD) should provide a valid comparison. Figure 5 shows histograms similar to Figure 2 without wet-radome correction (left) and with the correction (right). We observe that the wet-radome correction reduces the bias, improves the slope and improves the correlation. Because the MRR measures continuously, it is possible to match the observation times exactly, resulting in an improved correlation over the X-band intercomparison. The slope remains less than unity, possibly due to the differing attenuation correction schemes in use by the two radars or the uncompensated influences of vertical air motion on MRR observations.

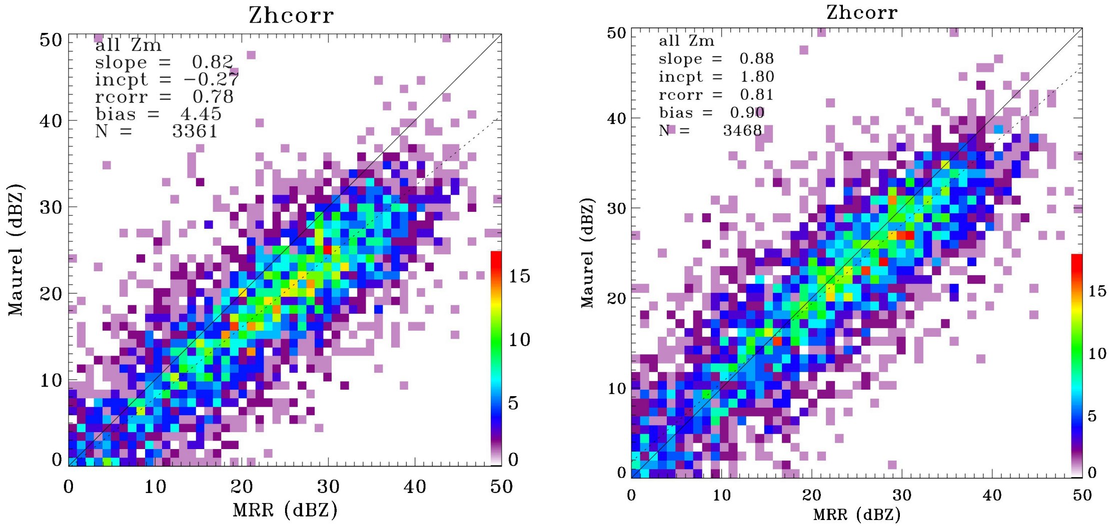


*Figure 5: Maurel vs. MRR reflectivity factor without wet radome correction (left) and with correction (right).*

## .4. Attenuation Correction via Differential Phase

The attenuation and differential attenuation correction scheme employed by Météo-France assumes a linear relationship between path-integrated attenuation (PIA) or path-integrated differential attenuation (PIDA) and the smoothed differential propagation phase according to:

$$PIA = 0.28\ \Phi_{DP}$$

$$PIDA = 0.04\ \Phi_{DP}.$$

The first relationship was derived experimentally using the Vial radar in combination with the nearby S-band radar at Nimes (Kabeche et al., 2010). The coefficient in the second relationship was not obtained experimentally, but was derived by dividing the coefficient for PIA by 7, consistent with other relationships taken from the literature (Bringi and Chandrasekar, 2001; Snyder et al., 2010).

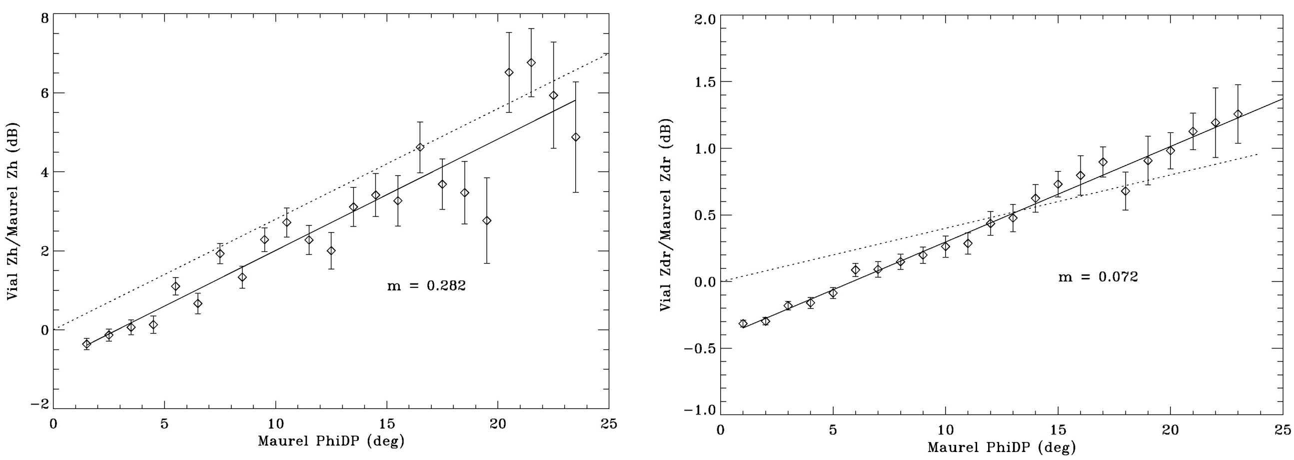


*Figure 6: On left, ratio of Vial/Maurel $Z_H$ (indicative of PIA from Maurel, see text) vs Maurel $\Phi_{DP}$. On right, ratios of $Z_{DR}$ (indicative of PIDA). Slopes of fits to data are indicated.*

To investigate the validity of these relationships, Figure 6 shows the mean ratios of $Z_H$ (Vial/Maurel) vs $\Phi_{DP}$ (Maurel) conditioned on the requirement that $\Phi_{DP}$ measured from Vial is less than 5 degrees. Thus, it is assumed that the Vial-measured reflectivity factor is subject to minimal PIA. In this case, the ordinate in Figure 6 may be interpreted as the PIA observed from Maurel. The aforementioned wet radome correction has been applied to the Maurel reflectivity observations to mitigate its impact. Fitting a line to the observed points yields a slope very close to 0.28, which is the result derived empirically. We note that the range of values of $\Phi_{DP}$ is somewhat limited, owing largely to the limited propagation distance between the radars and the comparison site (< 30 km).

The same approach can be used to evaluate the differential attenuation, also shown in Figure 6. In this case, the wet-radome attenuation correction is omitted as we assume both polarizations are subject to (nearly) the same attenuation. The resulting slope is approximately 0.07 which is nearly twice the value that is currently in use. If wet radome differential attenuation were present, it would most likely serve to reduce the observed slope (for example if rivulet flow on the radome impacted vertical polarization more strongly than horizontal). It is therefore suggested that a slope of 0.07 is more appropriate for the observations in the mountainous region of southeast France.

**Acknowledgment**

This work was done while the first author was on sabbatical at the Centre National de Recherches Météorologiques (CNRM) and Centre de Météorologie Radar, Direction des Systèmes d'Observation at Météo-France Toulouse. The authors and their organizations acknowledge the support of the European Union, the Provence-Alpes-Cote d'Azur Region, and the French Ministry of Ecology, Energy, Sustainable Development, and Sea who co-financed the RHYTMME project.

**References**

Bechini, R., V. Chandrasekar, R. Cremonini, and S. Lim, 2010: Radome attenuation at x-band radar operations. *ERAD 2010 – Sixth European Conference on Radar in Meteorology and Hydrology*, 6–10 Sept., Sibiu, Romania, 0346.

Bringi V. N, V. Chandrasekar, 2001: *Polarimetric Doppler Weather Radar: Principles and Applications*, Cambridge University Press.

Figueras i Ventura, J., A.-A. Boumahmoud, B. Fradon, P. Dupuy, P. Tabary, 2012: Long-term monitoring of French polarimetric radar data quality and evaluation of several polarimetric quantitative precipitation estimators in ideal conditions for operational implementation at C-band, *Q. J. R. Meteorol. Soc.,* early online release.

Kabeche, F., J. F. i Ventura, B. Fradon, A. A. Boumahmoud, A. Illingworth, and P. Tabary, 2010: Towards X-band polarimetric quantitative precipitation estimation in mountainous regions: The RHYTMME project. *ERAD 2010 – Sixth European Conference on Radar in Meteorology and Hydrology*, 6–10 Sept., Sibiu, Romania, 0113.

Kurri, M. and A. Huuskonen, 2008: Measurements of the transmission loss of a radome at different rain intensities. J. *Atmos. Oceanic. Tech.*, **25**, 1590–1599, doi:10.1175/2008JTECHA1056.1.

Snyder, J. C., H. B. Bluestein, G. Zhang, S. J. Frasier 2010: Attenuation Correction and Hydrometeor Classification of High-Resolution X-band Dual-Polarized Mobile Radar Measurements in Severe Convective Storms, *J. Atmos. Oceanic Tech.,* **27**, 1979—2001.

Trabal, J. M., I. Zawadski, and D. J. McLaughlin, 2008: A method to correct for wet radome attenuation in CASA radars by the use of a contiguous WSR-88D radar. *ERAD 2008 – Fifth European Conference on Radar in Meteorology and Hydrology*, 30 June–4 July, Helsinki, Finland, 0287.